Chemistry
A European
Journal

Chemistry
Europe
European Chemical
Societies Publishing

Title: Visible-Light-Enabled C-H Functionalization by a Direct Hydrogen Atom Transfer Uranyl Photocatalyst

Authors: Jipan Yu, Chongyang Zhao, Rong Zhou, Wenchao Gao, Shuai Wang, Kang Liu, Si-yu Chen, Kongqiu Hu, Lei Mei, Liyong Yuan, Zhifang Chai, Hanshi Hu, and Wei-Qun Shi

To be cited as: *Chem. Eur. J.* 10.1002/chem.202003431

Link to VoR: https://doi.org/10.1002/chem.202003431

WILEY-VCH

Chemistry - A European Journal 10.1002/chem.202003431

Uranyl Photocatalysis

Visible-Light-Enabled C-H Functionalization by a Direct Hydrogen Atom Transfer Uranyl Photocatalyst

Jipan Yu,[+],[a] Chongyang Zhao,[+],[b] Rong Zhou,[c] Wenchao Gao,[c] Shuai Wang,[a] Kang Liu,[a] Siyu Chen,[a] Kongqiu Hu,[a] Lei Mei,[a] Liyong Yuan,[a] Zhifang Chai,[a,d] Hanshi Hu[b] and Weiqun Shi*[a]*

Abstract: *Uranyl cation, as a powerful photocatalyst, at present, is seriously delayed compared to the development of its fundamental and structural chemistry. However, the characteristic of highly oxidative capability in the excited state {$[UO_2]^{2+*}$ (+ 2.6 V vs. SHE) combined with blue light (hv 380-500 nm) absorption and a long-lived fluorescence lifetime up to microseconds have revealed that uranyl cation approaches an ideal photocatalyst for visible-light-drvien organic transformations. Described herein is a successful utilization of uranyl nitrate photocatalyst which enables $C(sp^3)$-H activation and C-C bond formation through hydrogen atom transfer (HAT) under blue light irradiation. In particular, this operationally simple scenario provides an appropriate approach to synthesize diverse and valuable diarylmethane motifs. Mechanistic studies and DFT calculations provide insights into detailed mechanism of the photoinduced HAT pathway. The current research is suggestive of a general platform that could popularize promising uranyl photocatalytic performance.*

Introduction

Since the pioneering works of MacMillan[1] and Yoon,[2] photocatalytic organic synthesis, especially the one stimulated by visible light, has undergone a remarkable renaissance and witnessed dramatic developments for their mild and highly-efficient characteristics over the past decade.[3] While the functionalization of $C(sp^3)$-H bonds, as Holy Grails in modern Chemistry, has revolutionized the program of organic synthetic chemistry.[4] In this context, spectacular advances have been created in the direct functionalization of $C(sp^3)$-H bonds by visible light-enabled photocatalysis.[5] In general, photoinduced $C(sp^3)$-H bond activation strategy gives rise to advanced opportunities for organic functionalization, which involves HAT,[6] SET (Single Electron Transfer),[7] PCET (Proton-Coupled Electron Transfer)[8] or energy transfer[3a, 9] reactive routes. However, direct HAT catalyst, which directly abstract a hydrogen atom from substrate with the control of redox potentials, has been rarely investigated.[10] Additionally, a set system with relatively more positive oxidation potential and good compatibility suitable for operationally simple protocol by photo-promoted direct HAT process is more scarce. Thus, uranyl cation UO_2^{2+}, a relatively underdeveloped photocatalyst, endowed with visible light absorption, readily available and highly oxidizing excited state performance, arrested our attention.[11]

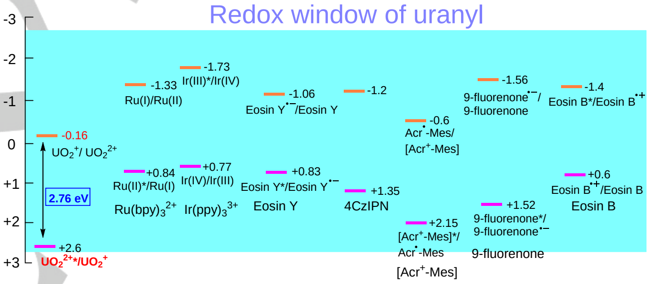

Figure 1. Redox potentials of uranyl with respect to commonly used photocatalysts

The available redox window of uranyl confirmed that the high oxidative ability for some redox-active substrates is greater than those of widely applied transition metal complexes[12] and organic dyes,[13] such as $Ru(bpy)_3^{2+}$ and eosin Y, etc. (Figure 1). The excited state, $[UO_2]^{2+}$*, with characteristic absorption of 380-500 nm blue right, adopts a long-lived fluorescence lifetime with the domain of microseconds and possesses a high oxidizability (E^o = + 2.6 V vs SHE).[11, 14] In the uranyl-catalyzed photocatalytic process, carbon-centered radical is usually generated through C-H bond homolytic cleavage (direct HAT process) by the oxygen site of the robust linear $[UO_2]^{2+}$*.[14a] In view of this promising reactivity and abundance of desirable characteristics, it appears that uranyl-catalyzed C-H functionalization with HAT procedure by visible light irradiation is anticipated. Among the few correlated reports, Sorensen's group developed a catalytic system for direct fluorination of unactivated $C(sp^3)$-H bonds by a uranyl photocatalyst.[15] In addition, Ravelli and co-workers described a practical protocol for the C-H to C-C bond conversion *via* uranyl photocatalysis upon visible-light irradiation.[16] Very recently, Jiang *et al.* investigated a selective and compatible oxidation of sulfides for the synthesis of sulfones and sulfoxides using $UO_2(OAc)_2{\cdot}2H_2O$ photocatalyst and molecular oxygen.[17] Concurrently, Arnold[18] and Takao[19] demonstrated a photocatalytic oxygenation of hydrocarbon in the presence of uranyl complex and visible light irradiation, respectively. In general, these remarkable but few contributions highlight the novelty and importance of unexplored

---

[*] Dr. J.-P. Yu, Dr. K.-Q. Hu, Dr. L. Mei, Dr. L.-Y. Yuan, Prof. Z.-F. Chai, Prof. W.-Q. Shi
Laboratory of Nuclear Energy Chemistry, Institute of High Energy Physics, Chinese Academy of Sciences, Beijing 100049 (China)
E-mail: shiwq@ihep.ac.cn; meil@ihep.ac.cn
Dr. C.-Y. Zhao, Prof. H.-S. Hu
Department of Chemistry & Key Laboratory of Organic Optoelectronics and Molecular Engineering of Ministry of Education, Tsinghua University, Beijing 100084 (China)
Prof. R. Zhou, Prof. W.-C. Gao
College of Chemistry and Chemical Engineering, Taiyuan University of Technology, Taiyuan 030024 (China)
Prof. Z.-F. Chai
Engineering Laboratory of Advanced Energy Materials, Ningbo Institute of Industrial Technology, Chinese Academy of Sciences, Ningbo 315201 (China)

[+] These authors contributed equally to this work.

Supporting information for this article is available on the WWW under http://dx.doi.org/10.1002/anie.202xxxxxx.

uranyl photochemistry. Therefore, we attempted to utilize this innovative scheme to activate the C-H bond through direct HAT photocatalysis, providing a convenient pathway for the synthesis of important bioactive molecules.

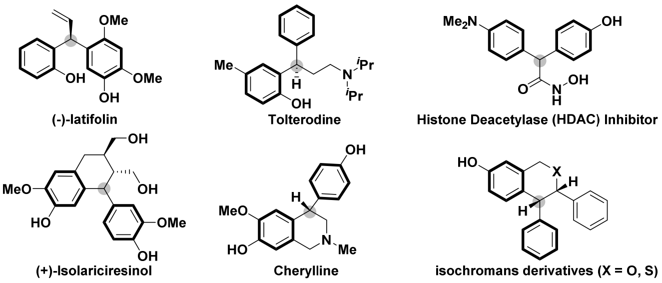

Figure 2. Selected bioactive compounds with a diarylmethane skeleton.

para-Quinone methides (*p*-QMs), as representative electrophilic acceptors, are unique feedstocks for the synthesis of value-added diarylmethane derivatives with multiple biological and pharmacological properties, such as antimicrobial, antiviral and anticancer (Figure 2).[20] Although 1,6-addition of *p*-QMs with various nucleophiles provide facile access to biologically active diarymethane derivatives have been reported,[21] the investigations on the pathway *via* visible light-promoted radical process of *p*-QMs are few.[22] Based on previous work, we reasoned that the radical alkylation of *p*-QMs through photo-induced direct HAT strategy might facilitate the delivery of diarylmethane derivatives with structural diversity. Accordingly, to address the above referred topics, herein we describe that uranyl ions can be employed as effective photocatalysts for the direct alkylation of *para*-quinone methides (*p*-QMs) under visible light irradiation.

Results and Discussion

To better assess the catalytic feasibility of this process, reactant **1a** and **2a** with various photosensitizers were employed as the benchmark substrate and alternative catalysts for optimization. As shown in Table 1, Ir(dF(CF$_3$)ppy)$_2$(dtbbpy)(PF$_6$) (**A**), Mes-Ac$^+$ClO$_4^-$ (**B**), 4CzIPN (**C**), 9-Fluorenone (**D**), [Ru(bpy)$_3$]Cl$_2$ (**E**), Eosin Y (**F**), Eosin B (**G**) and Uranyl Salt (**H**) were screened with THF as radical donor and CH_3CN as the solvent under argon atmosphere with irradiation of 5 W blue LED (entries 2-12), and we found that $UO_2(NO_3)_2\cdot 6H_2O$ afforded the highest catalytic efficiency to get the target product (**3a**) in 86% isolated yield (entry 9). The outcome indicated that $UO_2(NO_3)_2\cdot 6H_2O$ has an exclusive advantage over other photocatalysts for this catalytic system. The reaction did not occur in the absence of photocatalyst or without light (entry 1, 13). When the amount of $UO_2(NO_3)_2\cdot 6H_2O$ was increased from 5.0 mol% to 10 mol% (entry 16), similar yield of **3a** was obtained (compare entries 9 and 16), but lower reaction efficiency were observed with the decrease of amount of $UO_2(NO_3)_2\cdot 6H_2O$ (entries 14 and 15). Next, effect of solvents was surveyed, and CH_3CN was found to be a suitable solvent (compare entries 9, 17-21). Subsequently, we attempted to perform the reaction under air atmosphere, and the result showed that it was inferior to argon (compare entries 9 and 22). According to the results above, we believe the option that $UO_2(NO_3)_2\cdot 6H_2O$ as the photocatalyst in the presence of CH_3CN solvent is more suitable for the formation of intermolecular alkylated target adduct under visible light irradiation in Ar atmosphere.

Table 1. Optimization of conditions for alkylation of 4-benzylidene-2,6-di-tert-butylcyclohexa-2,5-dien-1-one (**1a**) leading to 2,6-di-tert-butyl-4-(phenyl(tetrahydrofuran-2-yl)methyl)phenol (**3a**).[a]

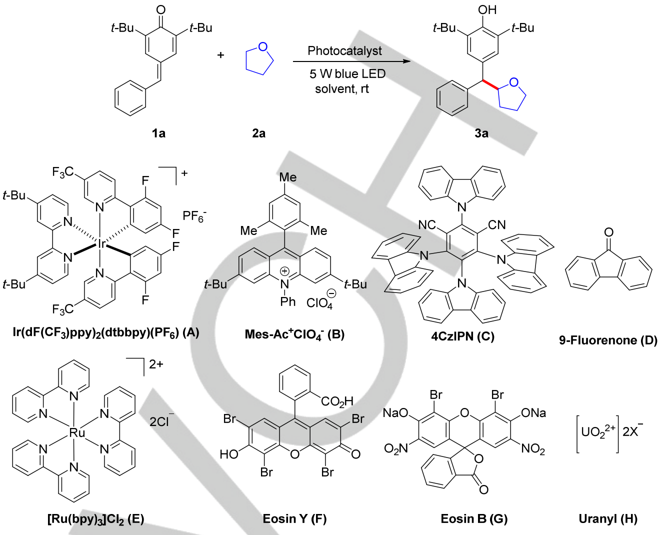

Entry	photocatalyst	Solvent	Yield (%)[b]
1		CH_3CN	0
2	**A** (5 mol%)	CH_3CN	trace
3	**B** (5 mol%)	CH_3CN	trace
4	**C** (5 mol%)	CH_3CN	56%
5	**D** (5 mol%)	CH_3CN	40%
6	**E** (5 mol%)	CH_3CN	trace
7	**F** (5 mol%)	CH_3CN	trace
8	**G** (5 mol%)	CH_3CN	trace
9	**$UO_2(NO_3)_2\cdot 6H_2O$ (5 mol%)**	**CH_3CN**	**86%**
10	$UO_2(OAc)_2\cdot 4H_2O$ (5 mol%)	CH_3CN	51%
11	$UO_2SO_4\cdot 4H_2O$ (5 mol%)	CH_3CN	57%
12	$UO_2(OTf)_2\cdot 6H_2O$ (5 mol%)	CH_3CN	66%
13[c]	$UO_2(NO_3)_2\cdot 6H_2O$ (5 mol%)	CH_3CN	0
14	$UO_2(NO_3)_2\cdot 6H_2O$ (1 mol%)	CH_3CN	30%
15	$UO_2(NO_3)_2\cdot 6H_2O$ (3 mol%)	CH_3CN	71%
16	$UO_2(NO_3)_2\cdot 6H_2O$ (10 mol%)	CH_3CN	84%
17	$UO_2(NO_3)_2\cdot 6H_2O$ (5 mol%)	CH_3COCH_3	82%
18	$UO_2(NO_3)_2\cdot 6H_2O$ (5 mol%)	EtOAc	73%
19	$UO_2(NO_3)_2\cdot 6H_2O$ (5 mol%)	DMSO	trace
20	$UO_2(NO_3)_2\cdot 6H_2O$ (5 mol%)	*o*-DCB	79%
21	$UO_2(NO_3)_2\cdot 6H_2O$ (5 mol%)	HFIP	trace
22[d]	$UO_2(NO_3)_2\cdot 6H_2O$ (5 mol%)	CH_3CN	60%

[a] Reaction conditions: under argon atmosphere, 4-benzylidene-2,6-di-tert-butylcyclohexa-2,5-dien-1-one (**1a**) (0.2 mmol, 1.0 equiv), catalyst (0.05 equiv), solvent (2.0 mL), room temperature (~ 25 °C), time (24 h) in a sealed Schlenk tube. [b] Isolated yield. [c] No light. [d] Under air condition. [e] DMSO = dimethylsulfoxide. *o*-DCB = 1,2-dichlorobenzene. HFIP = 1,1,1,3,3,3-Hexafluoro-2-propanol.

With the optimized visible-light-stimulated uranyl-catalyzed alkylation conditions in hand, we then explored the structural generality of *p*-QMs leading to diarylmethane derivatives under blue LED irradiation at the room temperature. As shown in Table 2, satisfactorily, the examined diverse substituents on *p*-QMs provided moderate to excellent yields. No evident difference was observed due to the electronic effect among the examined substrates. The substrates containing neutral methyl and electron-donating methoxyl groups gave the desired products in moderate to high yields (compounds **3b**, **3c**, **3d**, **3e** and **3f**). In addition, methylsulfide substrate could be used in the reaction to produce the corresponding product **3g** in 83% yield. Notably, naphthalene-substituted *p*-QMs as representative substrate provided the corresponding desired product **3h** with 38% yield. The uranyl-catalyzed alkylated reactions could tolerate some functional

Table 2. Substrate scope for the visible-light-promoted uranyl-catalyzed alkylation of 2,6-di-alkyl-4-(arylidene)cyclohexa-2,5-dien-1-one **1** with **2a**.[a]

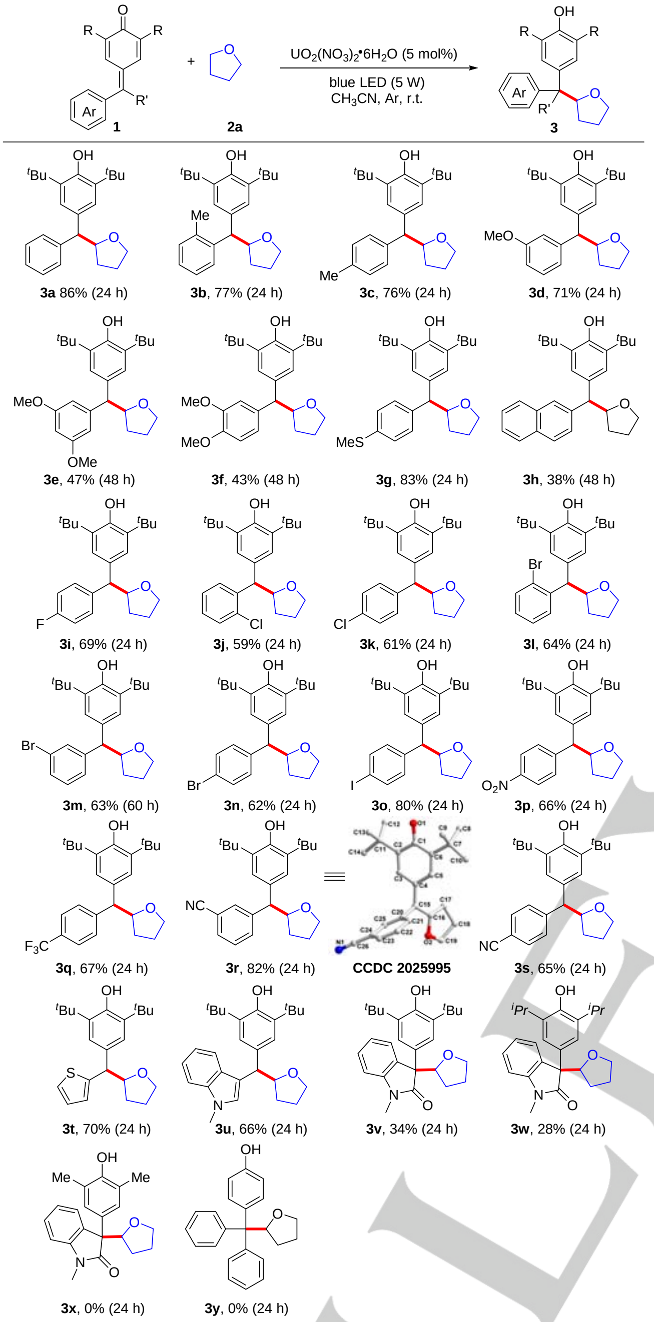

3a, 86% (24 h)
3b, 77% (24 h)
3c, 76% (24 h)
3d, 71% (24 h)
3e, 47% (48 h)
3f, 43% (48 h)
3g, 83% (24 h)
3h, 38% (48 h)
3i, 69% (24 h)
3j, 59% (24 h)
3k, 61% (24 h)
3l, 64% (24 h)
3m, 63% (60 h)
3n, 62% (24 h)
3o, 80% (24 h)
3p, 66% (24 h)
3q, 67% (24 h)
3r, 82% (24 h)
CCDC 2025995
3s, 65% (24 h)
3t, 70% (24 h)
3u, 66% (24 h)
3v, 34% (24 h)
3w, 28% (24 h)
3x, 0% (24 h)
3y, 0% (24 h)

[a] Reaction conditions: under argon atmosphere, 2,6-di-alkyl-4-(arylidene)cyclohexa-2,5-dien-1-one (**1**) (0.2 mmol, 1.0 equiv), $UO_2(NO_3)_2 \cdot 6H_2O$ (5 mg, 5 mol%), THF (**2a**) (1.0 mol, 5.0 equiv), CH_3CN (2.0 mL), room temperature (~25 °C), time (24~60 h) in a sealed tube. [b] Isolated yield.

groups in the substrates, including C-F bond (compound **3i**), C-Cl bonds (compounds **3i** and **3k**), C-Br bonds (compounds **3l**, **3m** and **3n**), C-I bond (compound **3o**), C-NO_2 bond (compound **3p**), C-CF_3 bond (compound **3q**) and C-CN bonds (compounds **3r** and **3s**). The structure of **3r** was further confirmed by X-ray single crystal diffraction. Halogen moieties, as the classical cross-coupling reagent for further structural transformation, were compatible with the reaction system along with the target products in satisfactory yields (**3i-3o**). In the meanwhile, heterocycles such as thiophene- and indole-derivative compounds **3t** and **3u** were also successfully obtained in decent yields (70% and 66%). To our delight, multi-substituted indolin-2-one derivatives **3v** and **3w** with the carbon quaternary center were constructed, especially isopropyl substituents **3w**, albeit with low yields. With respect to methyl- and H-substituted *p*-QMs, we found that no desired products **3x** and **3y** were isolated, suggesting that large steric hindrance group served as suitable precursors. Additionally, it must be pointed out that **3e, 3f, 3h** and **3m** require artificially prolonging reaction time to improve the reaction efficiency.

Table 3. Substrate scope for the visible-light-promoted uranyl-catalyzed alkylation of 4-benzylidene-2,6-di-tert-butylcyclohexa-2,5-dien-1-one **1a** with **2**.[a]

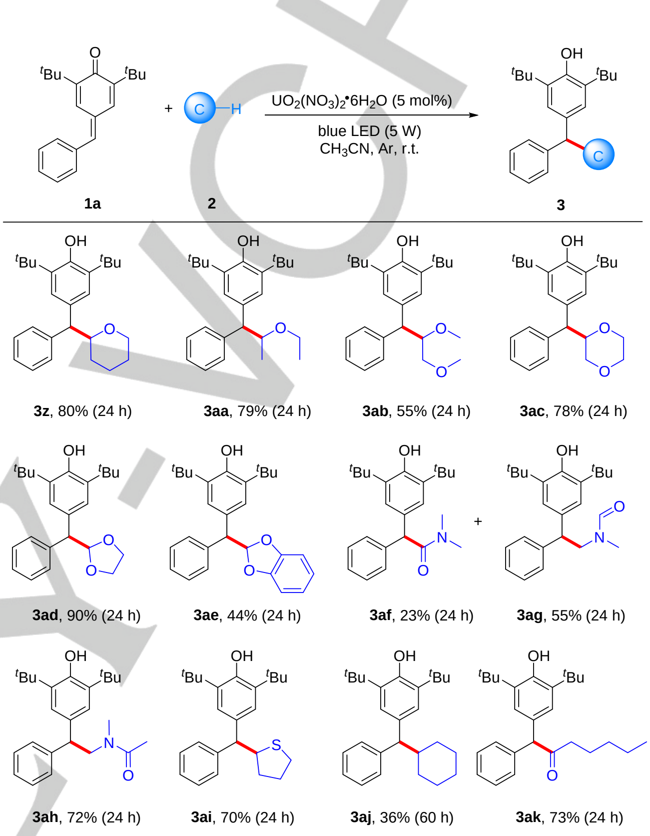

3z, 80% (24 h)
3aa, 79% (24 h)
3ab, 55% (24 h)
3ac, 78% (24 h)
3ad, 90% (24 h)
3ae, 44% (24 h)
3af, 23% (24 h)
3ag, 55% (24 h)
3ah, 72% (24 h)
3ai, 70% (24 h)
3aj, 36% (60 h)
3ak, 73% (24 h)

[a] Reaction conditions: under argon atmosphere, 4-benzylidene-2,6-di-tert-butylcyclohexa-2,5-dien-1-one (**1a**) (0.2 mmol, 1.0 equiv), $UO_2(NO_3)_2 \cdot 6H_2O$ (5 mg, 5 mol%), R-H (1.0 mol, 5.0 equiv), CH_3CN (2.0 mL), room temperature (~25 °C), time (24~60 h) in a sealed tube. [b] Isolated yield.

Then, apart from THF, we diverted our attention to other oxygenated radical precursors, including pyran, ether, diglyme, dioxane, 1,3-dioxolane and benzo[*d*][1,3]dioxole. Notably, the functionalization of C(sp^3)-H bonds in these oxygenated substrate occurred smoothly in moderate to excellent yields ranging 44-90% *via* the visible-light-driven generation of α-oxy radicals as well as α,α-dioxy radical (compounds **3z-3ae**). Dimethylformamide was chosen as H-donor to survey the reactive situation, whereas C-H activation was not regioselective, and produced the acylated and alkylated adducts **3af** and **3ag** with 23% and 55% yields, respectively. Interestingly, the protocol starting from *N,N*-dimethylacetamide (DMA) could be easily adapted to perform amidoalkyl rather than acylalkyl radical addition onto **2a**, which afforded the adduct **3ah** in 72% yield. And tetrahydrothiophene was functionalized toward the sulfuralkyl radical site with high regioselectivity to afford the desired product **3ai** in 70% yield. However, the functionalization of unactivated cyclalkane, such as hexane, occurred sluggishly with adduct **3aj** in only 36% yield even with longer reaction time. Importantly, adduct **3ak** was obtained in 73% yield with a complete regioselectivity *via* acyl radical procedure. According to this, we firmly believe that the present uranyl-catalyzed reactive pattern will be applicable extensively in the synthesis of pharmaceutically active molecules and/or organic functional materials containing diarylmethane moieties.

To demonstrate the synthetic practicability, a scale-up synthesis of **3a** was investigated as the example. As shown in Scheme 1, reaction of **1a** (3.74 mmol, 1.1 g) and THF under the standard conditions provided **3a** in 77% yield (1.05 g). Therefore, this method presents the effective applicability for the gram-scale synthesis of desired diarylmethane derivatives.

Scheme 1. Scale synthesis of 2,6-di-tert-butyl-4-(phenyl-tetrahydrofuran-2-yl)methyl)phenol.

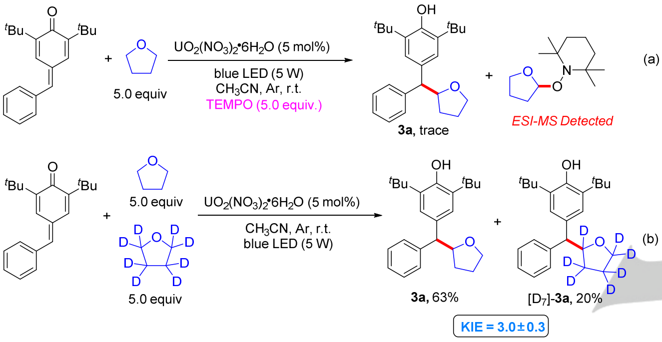

Scheme 2. (a) Radical trapping experiment. (b) Mechanistic studies on the kinetic isotope effect.

To elucidate the possible mechanism of visible-light-mediated uranyl-catalyzed alkylated reaction, Stern-Volmer fluorescence quenching experiments were performed (see Figures S2-S7 in the Supporting Information for the details). At first, we investigated the emission and excitation spectra of the photocatalyst $UO_2(NO_3)_2 \cdot 6H_2O$. A solution of $UO_2(NO_3)_2 \cdot 6H_2O$ (1.0 mM) in CH_3CN was chosen as the model. The fluorescence excitation spectrum was obtained with the detection wavelength of 480 nm (Figure S2), and the fluorescence emission spectrum was excited at 420 nm (excitation maximum of $UO_2(NO_3)_2 \cdot 6H_2O$) (Figure S3). As shown in Figure S2a, 467 nm, 484 nm, 505 nm, 528 nm and 554 nm finger peaks of fluorescence emission spectrum of $UO_2(NO_3)_2 \cdot 6H_2O$ was observed when it was excited at 420 nm, and the fluorescence intensity dramatically decrease with the addition of THF. Moreover, an energy transfer process between $UO_2(NO_3)_2 \cdot 6H_2O$ and THF was validated by fluorescence quenching experiments (see Figures S4-S5 for the details). Meanwhile, fluorescence emission spectra of $UO_2(NO_3)_2 \cdot 6H_2O$ with different concentration of 4-benzylidene-2,6-di-tert-butylcyclohexa-2,5-dien-1-one (**1a**) excited at 420 nm was carried out (Figure S2b). The outcome turns out that the excited state of uranyl nitrate could be quenched by the generation of the collision chelate complex through the C=O$\cdots$U coordination interaction (see Figures S6-S7 for details).[23]

In order to survey the reaction mechanism for the visible-light-enable uranyl-catalyzed alkylation process, a control experiment with the treament of 4-benzylidene-2,6-di-tert-butylcyclohexa-2,5-dien-1-one (**1a**) and THF (**2a**) in the presence of radical scavenger TEMPO (5 equiv) was conducted (Scheme 2a). The formation of **3a** was completely suppressed, and the radical adduct of THF-TEMPO was markedly formed and trapped by TEMPO in situ and detected by ESI-MS analysis. This observation severs as a compelling proof for the intermediate of THF radical be involved in this transformation process (Figure S8). Moreover, To further illustrate the C-H bond cleavage of THF in HAT process, the control deuterium isotopic labeling experiments were performed to verify the rate-determining step. The reaction was carried out in the present of 1:1 ratio of THF and D_8-THF as the partner, the experimental results showed that **3a** and [D_7]-**3a** were obtained with a significant kinetic isotope effect (KIE) value of 3.0 ± 0.3, revealing that the C-H bond cleavage occurred in the rate-determining step (Scheme 2b, see Figure S9 for details).

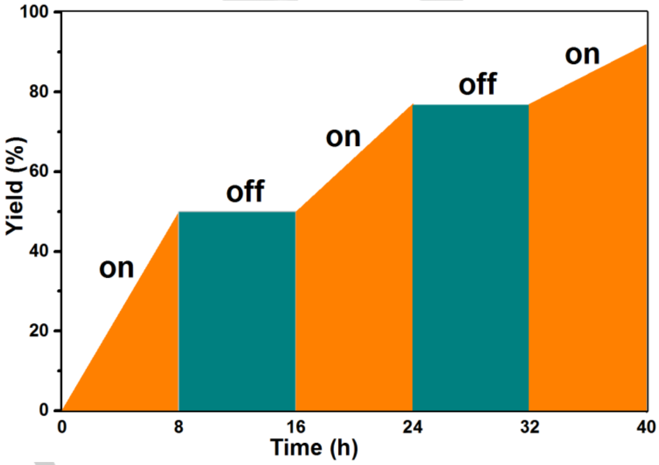

Figure 3. Profile of the formation of **1a** with the light turned on or off at regular intervals. Yields were determined by ^{1}H NMR spectroscopy with CH_2Br_2 as an internal standard.

Next, an on-off visible light irradiation experiment at regular intervals on the profile of the uranyl-catalyzed reaction yield was performed. The results implied that the continuous visible light irradiation was crucial for the transformation (Figure 3). In addition, the apparent quantum yield of the reaction was calculated to be 8.8%. It suggested that the radical program present a closed photocatalytic process without involvement of radical chain propagation (see details in the Supporting Information).

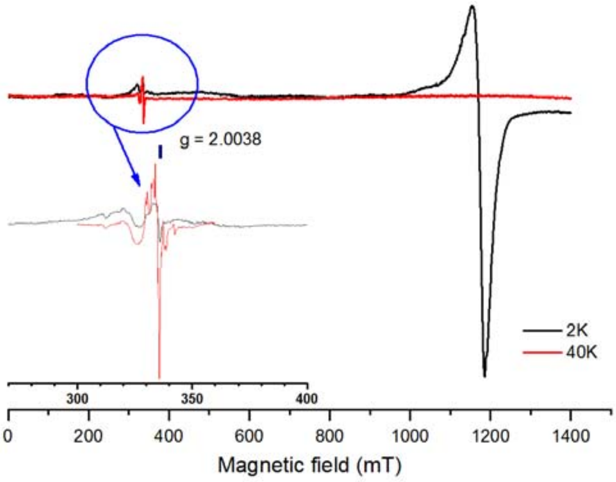

Figure 4. Experimental evidence for U(V)-oxo radical character in the U(V)-oxo moiety. The EPR spectra of $UO_2(NO_3)_2 \cdot 6H_2O$ dissolved in acetonitrile are recorded under the blue light at 2K and 40K respectively. The signals are magnified at the narrower range of the magnetic field in the inset.

In the origins of catalysis, the U(VI)-oxo valence tautomer is suggested as an important contributor to the excited state of U(V)-oxo radical intermediates under visible light irradiation.[14a, 23] However, experimental evidence for validating the proposals of such U(V)-oxo radical species has never been reported.[17] Thus, we sought to trap the reactive intermediate U(V)-oxo by EPR (Electron Paramagnetic Resonance) technique assisted by superfluid liquid helium at 2K. The EPR spectrum at 2K shows the characteristic signal of U(V) ion, which is produced from the excitation of $UO_2(NO_3)_2{\cdot}6H_2O$ by the irradiation of blue light (Figure 4). The *g*-values ($g_\perp$ = 0.570 and g_{II} = 2.085) indicate the axial symmetry for the coordination geometry of U(V) ion. On increasing the temperature to 40 K, the EPR signals are reduced except the one at g = 2.0038 which is growing independently and is not ascribed to the U(V) ion as a consequence. It is known that the 5f orbitals are more extended than 4f ones, leading to the covalent U-O bonds and the linear type of the form O-U-O for uranyl ion $(UO_2)^{2+}$, which has no unpaired electron and is therefore EPR silent.[24] $5f^1$ U(V) center with an oxygen radical species was formed via homolysis of U=O bonds under the irradiation of blue light. Taking the nitrate ligands coordinated in the equatorial plane into consideration, the symmetry of the crystal field about the O-U-O axis may be changed from C_∞ for uranyl ion to threefold or less for this compound in solution. In addition, there is possible structure deviation from linear O-U-O, caused by the reduction reaction under light. Both may mix the first excited states $^2F_{7/2}$ to the ground doublet $^2F_{5/2}$, activating the EPR lines.[24-25] For the U(V) species published in literatures, the *g*-value are found between 0.7 and 2.1, while for neptunyl ion ($(NpO_2)^{2+}$, $5f^1$) the *g*-value are $g_\perp$ = 0.205 and g_{II} = 3.405.[26] The above EPR results confirmed that the generation of U(V)-oxo species from U(VI)-oxo precursor is considered as the initial step of photo-induced reaction.

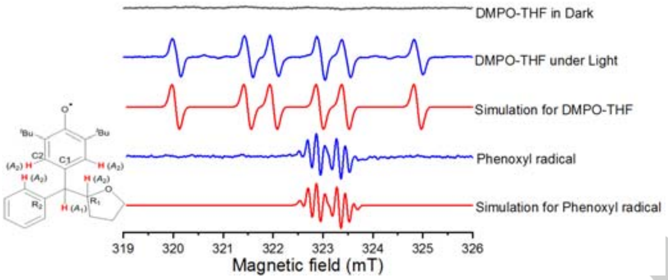

Figure 5. The X-band EPR spectra of a mixture of $UO_2(NO_3)_2{\cdot}6H_2O$ (cat; 5 mol%), THF (**2a**, 50 mM) and 5,5-dimethyl-1-pyrroline *N*-oxide (DMPO; 50 mM) before and after the irradiation of UV-Vis light. The blue line at bottom represents the EPR spectrum of the phenoxyl radical produced in the reaction of $UO_2(NO_3)_2{\cdot}6H_2O$ (cat; 5 mol %), THF (**2a**, 50 mM) and **1a** (10 mM) under the irradiation. The *g*-value and hyperfine splitting constants from the adduct of the THF radical and DMPO and the phenoxyl radical are obtained by simulation with Easyspin.[27]

Meanwhile, we investigated types of the radicals produced during different conditions by electron paramagnetic resonance (EPR) technique (Figure 5). $UO_2(NO_3)_2{\cdot}6H_2O$ (cat; 5 mol %), THF (**2a**, 50 mM) and 5,5-dimethyl-1-pyrroline *N*-oxide (DMPO, *ca.* 100 mM after mixing) as the radical trapper were mixed in solvent CH_3CN and transferred to capillaries. Then the EPR spectra of the mixture were recorded under different conditions. No radical signal was observed without irradiation of light; in contrast, a sextet signal with a *g* value of 2.006 and hyperfine splitting constants (A_N = 1.445 mT and A_H = 1.963 mT) was obtained under irradiation with UV-Vis light, indicating a product of carbon-centered radical which is probably ascribed to the adduct of DMPO by THF **2a** (Figure 5). Considering that the phenoxyl radical as the possible intermediate is stable enough for the observation of EPR signal, the EPR spectra were recorded when the CH_3CN solution of $UO_2(NO_3)_2{\cdot}6H_2O$ (cat; 5 mol%), THF (**2a**, 50 mM) and **1a** (10 mM) were reacted under the in-situ irradiation. The *g*-value (g = 2.0028) and hyperfine splitting constants (A_1 = 0.4103 mT, A_2 = 0.1606 mT) of the reaction intermediate were derived by simulation. The smaller constant A_2 may be originated from four hydrogen nuclei poccessing identical hyperfine splitting constants.

The lager hyperfine splitting constant A_1 may be originated from the hydrogen nucleus from the methyne at the '*p*' position of the phenol ring. From the DFT calculation result (see below), the *π* molecular orbitals are found to contain the 1.09% contribution from the atom orbitals for hydrogen of methyne but the contribution no more than 0.12% from other H atoms, indicating the overlap between the C-H bond of methyne and the *π* molecular orbitals and the delocalization of *π*-spin on this hydrogen atom. Furthermore, according to the formula in supplementary information and the spin density (21.77%) of C1 from DFT calculation, the dihedral angle between the C-H bond of methyne and the normal to the phenol ring is estimated as 71°.[28] Contrary to the C-H bond of methyne, the double of C-H bonds on '*m*' position are almost parallel to the phenol ring, leading to a relatively small hyperfine splitting constant (A_2) originated from the spin polarization of the C2 atom. The other two hydrogen atoms with the constants of A_2 may be the H atoms of furan ring and of the phenyl substituted to methyne. Pratically, the relatively large hyperfine splitting constant for the hydrogen of methyne is also found for galvinoxyl radical, an analogue to the phenoxyl radical in this work.[28] The *π*-spin character and the two identical H atoms at '*m*' position of phenol ring illustrate the resonance form II (see below, Scheme 3) is the largest contributor among the three possible resonance forms. In other work, the crystal structure of the 2,4,6-tri-*tert*-butylphenoxyl radical (^{t}Bu$_3$ArO·) proves to be the form with the radical on the carbon atom linking to the *p*-*tert*-butyl.[29]

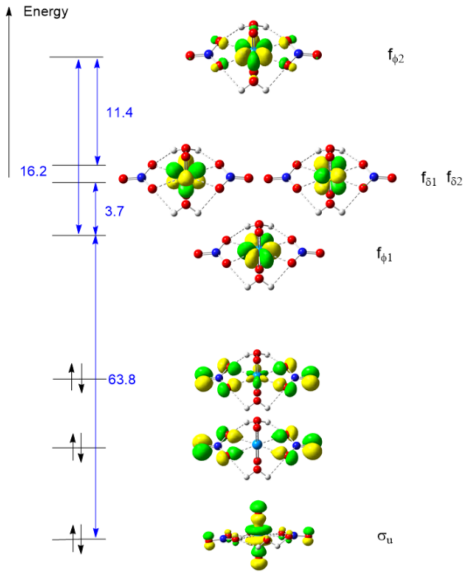

Figure 6. The orbital levels for $UO_2(NO_3)_2{\cdot}6H_2O$ calculated at PBE0/6-31G(d,p)/SDD level in combination with continuum solvation model IEFPCM. The unit of orbital energy level gaps is kcal/mol.

To explore mechanism of the visible light-mediated uranyl-catalyzed alkylated reaction, a DFT calculation could provide exhaustive detail about the reaction intermediates and mechanisms. Refer to the photophysics process studied by Chen[23], the uranyl of triplet is responsible for the abstraction of hydrogen atom in THF. It has the electronic configuration $^3(\sigma_u f_{\delta 1})$. The DFT calculations reproduce the energic order $^3(\sigma_u f_{\delta 1}) < {}^3(\sigma_u f_{\delta 2}) < {}^3(\sigma_u f_{\phi 1})$ of triplet uranyl calculated by CASPT2[23]. This indicates the reliability of our DFT calculations. The nearly equal two axial U-O bond with the length difference by 0.001Å in triplet LMCT uranyl indicates the averaged arrangement of spin densities on the two oxo ligand. Indeed, the spin densities of two oxo ligand are 0.205 and 0.209. THF encounters the uranyl and then forms the complex by hydrogen bound between the proton in one of equatorial water molecules and oxygen atom in THF. Figure 6 shows the molecular orbital of the uranyl of singlet state. In the HAT transition state, the Mulliken spin density of carbon in THF is 0.069, the C-H bond length is 1.121Å slightly longer than its usually state, which reflects this transition state resembles the reactant complex. However, the arrangement of the spin densities on the oxo ligands are not averaged, the oxo abstracting hydrogen atom in THF is centralized more spin density than the other oxo by 0.270. The potential energy curve for the reaction is shown in Figure 7, HAT process is accessible at room temperature due to the low free energy barrier of 3.10 kcal/mol.

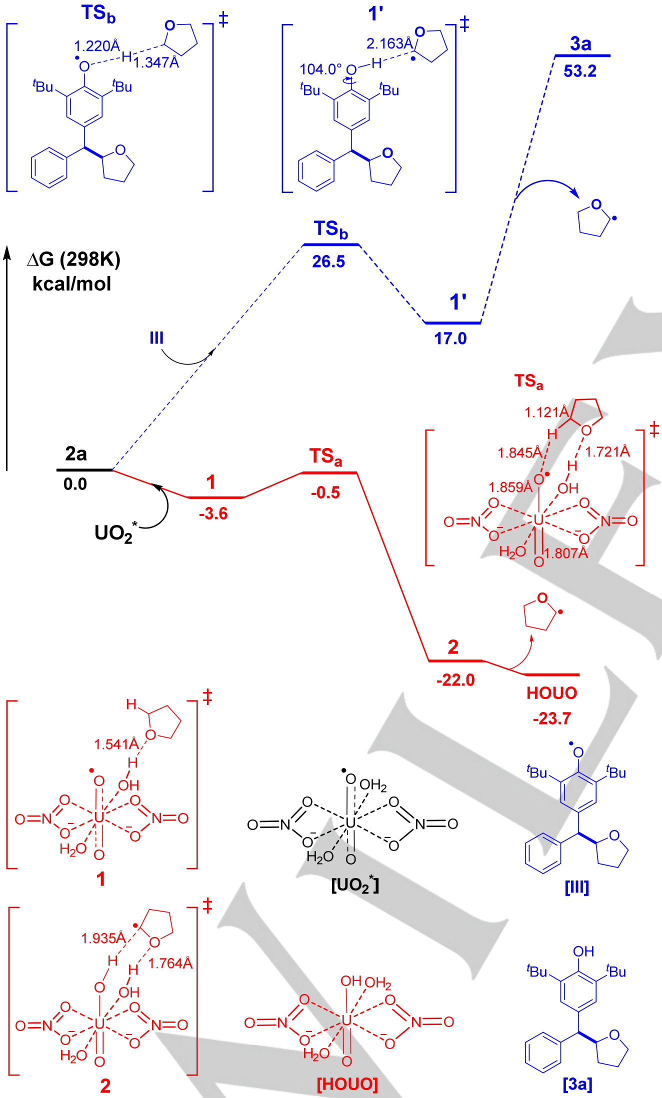

Figure 7. The potential energy profile of HAT process of THF by LMCT uranyl species and phenoxy radical species III.

According to the control experiments above and previous references,[17] a possible mechanism for the visible-light-mediated uranyl-catalyzed alkylated pathway is proposed in Scheme 3. At first, photosensitizer, uranyl cation (UO_2^{2+}), is transformed into its triplet excited state UO_2^{2+}* under irradiation of visible light. But accompanying generates active oxygen radical U(V) species with high oxidative potential through ligand to metal charge transfer (LMCT). Next, a carbon-centered radical **I** was generated by activated radical U(V) species through a HAT process, and radical U(V) species abstract a H atom to produce U(V)O(OH)$^{2+}$. In the alkylation process, nucleophilic addition of radical **I** to 4-benzylidene-2,6-di-tert-butylcyclohexa-2,5-dien-1-one **1a** provide a transient radical adduct **II**. Since the largest resonance contribution, **II** could be transformed into phenoxy radical species **III**, which is capable of oxidizing the reduced form of U(V)O(OH)$^{2+}$ to deliver anion **IV** while regenerating the photocatalyst UO_2^{2+}. Deuterium labeling experiments indicated that phenoxyl anion **IV** would most likely abstract a free hydrogen proton from the trace water in the reaction system. Finally, protonation of intermediate **IV** affords the target molecule **3a**. The process of path a exhibited a low free energy barrier based on the DFT calculation (Figure 7). Meanwhile, radical III and another THF molecule might undergo a short cut to deliver the desired alkylation product 3a, while the result based on the DFT calculation showed a high free energy barrier (26.5 kcal mol-1) (path b). Therefore, we were able to safely exclude the possibility of path b at current stage (Figure 7).

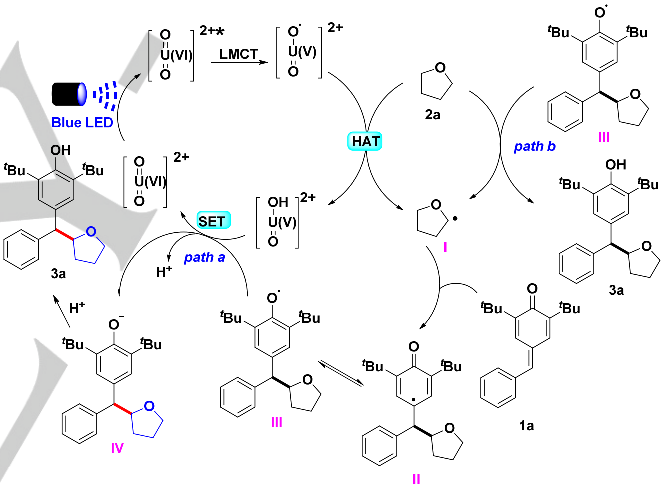

Scheme 3. A possible mechanism for the uranyl-catalyzed alkylation of 4-arylidene-cyclohexa-2,5-dien-1-one derivatives under visible light irradiation.

Conclusion

In summary, we have developed an efficient and reliable visible light-mediated uranyl-catalyzed C-H alkylation reaction through HAT process at room temperature. A variety of diarylmethane derivatives with important potential pharmaceutical value were obtained in reasonable yields by using our method. The transformation accommodates a broad substrate scope, available raw feedstocks, operational simplicity, green protocol and gratified scale-up synthesis. Mechanistic studies and DFT calculations reveal that the HAT process is triggered by virtue of the high oxidative nature of the oxygen of uranyl species upon light excitation, generating a radical intermediate, which undergoes addition/isomerization/hydrogen migration process in a synchronously concerted manner. Furthermore, we believe that available photocatalyst uranyl cation induced radical reaction *via* HAT process represents a forceful and advanced strategy and will find wide applications for C-H activation. Other challenging organic transformation catalyzed by excellent candidate UO_2^{2+}, are currently under investigated in our lab.

Experimental Section

To a reaction tube (10 mL) equipped with a magnetic stir bar, 2,6-di-alkyl-4-(arylidene)cyclohexa-2,5-dien-1-one (0.2 mmol), alkylated reagent (1.0 mmol, 5.0 equiv.), $UO_2(NO_3)_2 \cdot 6H_2O$ (5.0 mol %), CH_3CN (2 mL) were added, then the system was sealed and exchange with Ar for about 3 times with water pump. The reaction mixture was stirred (1000 rpm) and irradiated by blue light in paralleled reactor (SCI-PCRS-2-220, Anhui kemi Machinery Technology Co., Ltd) at room temperature for 24 h or 60 h. After the reaction was completed, the reaction solution was concentrated under reduced pressure to yield crude product, which was purified by flash chromatography (silica gel, petroleum ether/ethyl acetate) to give the desired product **3**.

Acknowledgements

The authors are appreciative of financial support provided by the National Science Fund for Distinguished Young Scholars (No. 21925603), the National Natural Science Foundation of China (No. 21806167) and the Science Challenge Project (TZ2016004) on the project. A portion of this work was performed on the Steady High Magnetic Field Facilities, High Magnetic Field Laboratory, CAS. We also acknowledged Prof. Haijun Yang, Prof. Min Jiang and Dr. Ye Bi from Department of Chemistry, Tsinghua University for valuable suggestions and experimental assistance.

Conflict of interest

The authors declare no conflict of interest.

Keywords: uranyl cation • photocatalysis • hydrogen atom transfer • C-H activation • diarylmethane derivatives

[1] D. A. Nicewicz, D. W. C. MacMillan, *Science* **2008**, *322*, 77-80.

[2] M. A. Ischay, M. E. Anzovino, J. Du, T. P. Yoon, *J. Am. Chem. Soc.* **2008**, *130*, 12886-12887.

[3] a) F. Strieth-Kalthoff, M. J. James, M. Teders, L. Pitzer, F. Glorius, *Chem. Soc. Rev.* **2018**, *47*, 7190-7202; b) J. Twilton, C. Le, P. Zhang, M. H. Shaw, R. W. Evans, D. W. C. MacMillan, *Nat Rev Chem* **2017**, *1*, 1-18; c) M. Parasram, V. Gevorgyan, *Chem. Soc. Rev.* **2017**, *46*, 6227-6240; d) Y. Chen, L. Q. Lu, D. G. Yu, C. J. Zhu, W. J. Xiao, *Sci. China .Chem* **2019**, *62*, 24-57.

[4] a) T. G. Saint-Denis, R. Y. Zhu, G. Chen, Q. F. Wu, J. Q. Yu, *Science* **2018**, *359*, 759-770; b) F. L. Zhang, K. Hong, T. J. Li, H. Park, J. Q. Yu, *Science* **2016**, *351*, 252-256; c) J. F. Hartwig, *Acc. Chem. Res.* **2017**, *50*, 549-555.

[5] a) J. D. Cuthbertson, D. W. C. MacMillan, *Nature* **2015**, *519*, 74-77; b) J. L. Jeffrey, J. A. Terrett, D. W. C. MacMillan, *Science* **2015**, *349*, 1532-1536; c) M. H. Shaw, V. W. Shurtleff, J. A. Terrett, J. D. Cuthbertson, D. W. C. MacMillan, *Science* **2016**, *352*, 1304-1308; d) S. Mukherjee, B. Maji, A. Tlahuext-Aca, F. Glorius, *J. Am. Chem. Soc.* **2016**, *138*, 16200-16203; e) I. Kim, B. Park, G. Kang, J. Kim, H. Jung, H. Lee, M. H. Baik, S. Hong, *Angew. Chem. Int. Ed.* **2018**, *57*, 15517-15522; *Angew. Chem.* **2018**, *130*, 15743-15748; f) J. Zhang, D. Liu, S. Liu, Y. Y. Ge, Y. Lan, Y. Y. Chen, *iscience* **2020**, *23*, 10075.

[6] a) S. Rohe, A. O. Morris, T. McCallum, L. Barriault, *Angew. Chem. Int. Ed.* **2018**, *57*, 15664-15669; *Angew. Chem.* **2018**, 130, 15890-15895; b) H. Zhao, J. Jin, *Org. Lett.* **2019**, *21*, 6179-6184; c) H. P. Deng, Q. Zhou, J. Wu, *Angew. Chem. Int. Ed.* **2018**, *57*, 12661-12665; *Angew. Chem.* **2018**, *130*, 12843-12847; d) L. Capaldo, D. Ravelli, *Eur. J. Org. Chem.* **2017**, 2056-2071; e) S. Protti, M. Fagnoni, D. Ravelli, *Chemcatchem* **2015**, *7*, 1516-1523.

[7] a) Y. Y. Loh, K. Nagao, A. J. Hoover, D. Hesk, N. R. Rivera, S. L. Colletti, I. W. Davies, D. W. C. MacMillan, *Science* **2017**, *358*, 1182-1187; b) R. Zhou, H. W. Liu, H. R. Tao, X. J. Yu, J. Wu, *Chem. Sci.* **2017**, *8*, 4654-4659; c) H. P. Deng, X. Z. Fan, Z. H. Chen, Q. H. Xu, J. Wu, *J. Am. Chem. Soc.* **2017**, *139*, 13579-13584; d) H. W. Liu, L. S. Ma, R. Zhou, X. B. Chen, W. H. Fang, J. Wu, *ACS Catal.* **2018**, *8*, 6224-6229; e) J. Fang, W. L. Dong, G. Q. Xu, P. F. Xu, *Org. Lett.* **2019**, *21*, 4480-4485.

[8] a) C. M. Morton, Q. L. Zhu, H. Ripberger, L. Troian-Gautier, Z. S. D. Toa, R. R. Knowles, E. J. Alexanian, *J. Am. Chem. Soc.* **2019**, *141*, 13253-13260; b) G. J. Choi, Q. L. Zhu, D. C. Miller, C. J. Gu, R. R. Knowles, *Nature* **2016**, *539*, 268-271; c) D. C. Miller, K. T. Tarantino, R. R. Knowles, *Top Curr Chem* **2016**, *374*.

[9] Q. Q. Zhou, Y. Q. Zou, L. Q. Lu, W. J. Xiao, *Angew. Chem. Int. Ed.* **2019**, *58*, 1586-1604; *Angew. Chem.* **2019**, *131*, 1600-1619.

[10] a) X. Z. Fan, J. W. Rong, H. L. Wu, Q. Zhou, H. P. Deng, J. Da Tan, C. W. Xue, L. Z. Wu, H. R. Tao, J. Wu, *Angew. Chem. Int. Ed.* **2018**, *57*, 8514-8518; *Angew. Chem.* **2018**, *130*, 8650-8654; b) I. B. Perry, T. F. Brewer, P. J. Sarver, D. M. Schultz, D. A. DiRocco, D. W. C. MacMillan, *Nature* **2018**, *560*, 70-75; c) V. I. Supranovich, V. V. Levin, A. D. Dilman, *Org. Lett.* **2019**, *21*, 4271-4274; d) A. Dewanji, P. E. Krach, M. Rueping, *Angew. Chem. Int. Ed.* **2019**, *58*, 3566-3570; *Angew. Chem.* **2019**, *131*, 3604-3608; e) Y. L. Kuang, K. Wang, X. C. Shi, X. Q. Huang, E. Meggers, J. Wu, *Angew. Chem. Int. Ed.* **2019**, *58*, 16859-16863; *Angew. Chem.* **2019**, *131*, 17015-17019.

[11] H. D. Burrows, S. J. Formosinho, M. D. G. Miguel, F. P. Coelho, *Journal of the Chemical Society, Faraday Transactions 1: Physical Chemistry in Condensed Phases* **1976**, *72*, 163-171.

[12] a) C. K. Prier, D. A. Rankic, D. W. C. MacMillan, *Chem. Rev.* **2013**, *113*, 5322-5363; b) J. A. Leitch, T. Rossolini, T. Rogova, J. A. P. Maitland, D. J. Dixon, *ACS Catal.* **2020**, *10*, 2009-2025.

[13] a) N. A. Romero, D. A. Nicewicz, *Chem. Rev.* **2016**, *116*, 10075-10166; b) T. Y. Shang, L. H. Lu, Z. Cao, Y. Liu, W. M. He, B. Yu, *Chem. Commun.* **2019**, *55*, 5408-5419; c) I. A. MacKenzie, L. Wang, N. P. R. Onuska, O. F. Williams, K. Begam, A. M. Moran, B. D. Dunietz, D. A. Nicewicz, *Nature.* **2020**, *580*, 76-80; d) G. L. Eakinsa, J. S. Alfordb, B. J. Tiegsa, B. E. Breyfoglea, C. J. Stearmana. *J. Phys. Org. Chem.* **2011**, *24*, 1119-1128; e) M. Majek, A. Jacobi von Wangelin, *Acc. Chem. Res.* **2016**, *49*, 2316-2327.

[14] a) Y. Li, J. Su, E. Mitchell, G. Q. Zhang, J. Li, *Sci. China .Chem* **2013**, *56*, 1671-1681; b) R. Ghosh, J. A. Mondal, H. N. Ghosh, D. K. Palit, *J. Phys. Chem. A* **2010**, *114*, 5263-5270; c) R. G. Denning, *The Journal of Physical Chemistry A* **2007**, *111*, 4125-4143; d) Y. Mao, A. Bakac, *J. Phys. Chem.* **1996**, *100*, 4219-4223; e) W. D. Wang, A. Bakac, J. H. Espenson, *Inorg. Chem.* **1995**, *34*, 6034-6039; f) C. K. Jorgensen, R. Reisfeld, *Struct. Bonding (Berlin)* **1982**, *50*, 121-171; g) H. D. Burrows, T. J. Kemp, *Chem. Soc. Rev.* **1974**, *3*, 139-165.

[15] a) J. G. West, T. A. Bedell, E. J. Sorensen, *Angew. Chem. Int. Ed.* **2016**, *55*, 8923-8927; *Angew. Chem.* **2016**, *128*, 9069-9073; b) C. N. Neumann, T. Ritter, *Nat. Chem.* **2016**, *8*, 822-823.

[16] L. Capaldo, D. Merli, M. Fagnoni, D. Ravelli, *ACS Catal.* **2019**, *9*, 3054-3058.

[17] Y. M. Li, S. A. E. A. Rizvi, D. Q. Hu, D. W. Sun, A. H. Gao, Y. B. Zhou, J. Li, X. F. Jiang, *Angew. Chem. Int. Ed.* **2019**, *58*, 13499-13506; *Angew. Chem.* **2019**, *131*, 13633-13640.

[18] P. L. Arnold, J. M. Purkis, R. Rutkauskaite, D. Kovacs, J. B. Love, J. Austin, *Chemcatchem* **2019**, *11*, 3786-3790.

[19] T. Mashita, S. Tsushima, K. Takao, *Acs Omega* **2019**, *4*, 7194-7199.

[20] a) M. Recanatini, A. Cavalli, P. Valenti, *Med. Res. Rev.* **2002**, *22*, 282-304; b) H. A. I. Yoshihara, J. W. Apriletti, J. D. Baxter, T. S. Scanlan, *Bioorg. Med. Chem. Lett.* **2001**, *11*, 2821-2825; c) R. B. An, G. S. Jeong, Y. C. Kim, *Chem. Pharm. Bull.* **2008**, *56*, 1722-1724; d) J. Liu, E. T. Birzin, W. D. Chan, Y. T. Yang, L. Y. Pai, C. DaSilva, E. C. Hayes, R. T. Mosley, F. DiNinno, S. P. Rohrer, J. M. Schaeffer, M. L. Hammond, *Bioorg. Med. Chem. Lett.* **2005**, *15*, 715-718.

[21] a) W. D. Chu, L. F. Zhang, X. Bao, X. H. Zhao, C. Zeng, J. Y. Du, G. B. Zhang, F. X. Wang, X. Y. Ma, C. A. Fan, *Angew. Chem. Int. Ed.* **2013**, *52*, 9229-9233; *Angew. Chem.* **2013**, *125*, 9399-9403; b) L. Caruana, F. Kniep, T. K. Johansen, P. H. Poulsen, K. A. Jorgensen, *J. Am. Chem. Soc.* **2014**, *136*, 15929-15932; c) Y. Z. Lou, P. Cao, T. Jia, Y. L. Zhang, M. Wang, J. Liao, *Angew. Chem. Int. Ed.* **2015**, *54*, 12134-12138; *Angew. Chem.* **2015**, *127*, 12302-12306; d) C. Jarava-Barrera, A. Parra, A. Lopez, F. Cruz-Acosta, D. Collado-Sanz, D. J. Cardenas, M. Tortosa, *ACS Catal.* **2016**, *6*, 442-446; e) N. Dong, Z. P. Zhang, X. S. Xue, X. Li, J. P. Cheng, *Angew. Chem. Int. Ed.* **2016**, *55*, 1460-1464; *Angew. Chem.* **2016**, *128*, 1482-1486; f) X.-Y. Chen, K. Zhao, Q. Liu, Y. Zhi, J. Ward, K. Rissanen, D. Enders, *CCS Chemistry* **2019**, *1*, 261-267; g) Z. L. Liu, H. F. Xu, T. F. Yao, J. L. Zhang, L. Liu,

Org. Lett. **2019**, *21*, 7539-7543; h) D. Wang, Z. F. Song, W. J. Wang, T. Xu, *Org. Lett.* **2019**, *21*, 3963-3967; i) Y. Y. Shen, J. F. Qi, Z. J. Mao, S. L. Cui, *Org. Lett.* **2016**, *18*, 2722-2725; j) M. L. Ke, Q. L. Song, *Adv. Synth. Catal.* **2017**, *359*, 384-389; k) Z. P. Zhang, N. Dong, X. Li, *Chem. Commun.* **2017**, *53*, 1301-1304; l) N. Molleti, J. Y. Kang, *Org. Lett.* **2017**, *19*, 958-961; m) P. Goswami, G. Singh, R. V. Anand, *Org. Lett.* **2017**, *19*, 1982-1985; n) R. Li, Y. Chen, K. Jiang, F. Y. Wang, C. F. Lu, J. Q. Nie, Z. X. Chen, G. C. Yang, Y. C. Chen, Y. Zhao, C. Ma, *Chem. Commun.* **2019**, *55*, 1217-1220.

[22] a) Y. N. Zhao, Y. C. Luo, Z. Y. Wang, P. F. Xu, *Chem. Commun.* **2018**, *54*, 3993-3996; b) Q. Y. Wu, G. Z. Ao, F. Liu, *Org. Chem. Front.* **2018**, *5*, 2061-2064; c) S. G. More, G. Suryavanshi, *Org. Biomol. Chem.* **2019**, *17*, 3239-3248; d) J. Guo, G. B. Huang, Q. L. Wu, Y. Xie, J. Weng, G. Lu, *Org. Chem. Front.* **2019**, *6*, 1955-1960; e) W. Zhang, C. Yang, Z. P. Zhang, X. Li, J. P. Cheng, *Org. Lett.* **2019**, *21*, 4137-4142.

[23] L. L. Wu, X. Y. Cao, X. B. Chen, W. H. Fang, M. Dolg, *Angew. Chem. Int. Ed.* **2018**, *57*, 11812-11816.

[24] A. Abragam, B. Bleaney, *Electron paramagnetic resonance of transition ions*, OUP Oxford, **1970**.

[25] R. A. Layfield, M. Murugesu, *Lanthanides and actinides in molecular magnetism*, John Wiley & Sons, **2015**.

[26] a) W. W. Lukens, N. M. Edelstein, N. Magnani, T. W. Hayton, S. Fortier, L. A. Seaman, *J. Am. Chem. Soc.* **2013**, *135*, 10742-10754; b) M. L. Gilchrist, J. A. Ball, D. W. Randall, R. D. Britt, *Proc. Natl. Acad. Sci. U. S. A.* **1995**, *92*, 9545-9549.

[27] S. Stoll, A. Schweiger, *J Magn Reson* **2006**, *178*, 42-55.

[28] A. Watanabe, N. Noguchi, A. Fujisawa, T. Kodama, K. Tamura, O. Cynshi, E. Niki, *J. Am. Chem. Soc.* **2000**, *122*, 5438-5442.

[29] V. W. Manner, T. F. Markle, J. H. Freudenthal, J. P. Roth, J. M. Mayer, *Chem. Commun.* **2008**, 256-258.

Entry for the Table of Contents

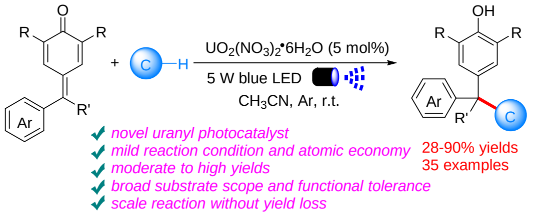

An efficient and convenient C-H activation strategy through direct HAT process for synthesis of highly value-added diarylmethane derivatives from *p*-QMs was realized by combining a uranyl photocatalyst with visible light irradiation. EPR experiments and DFT calculations revealed that the formation of U(V)-O$^{\cdot}$ species by reduction of U(VI)=O under visible light is responsible for the initial step of photo-induced reaction.